EDGEWOOD

CHEMICAL BIOLOGICAL CENTER

U.S. ARMY RESEARCH, DEVELOPMENT AND ENGINEERING COMMAND

ECBC-CR-092

EVAPORATION INTO COUETTE FLOW

James E. Danberg

SCIENCE APPLICATIONS INTERNATIONAL CORPORATION
Abingdon, MD 21009

January 2008

ABERDEEN PROVING GROUND, MD 21010-5424

Disclaimer

The findings in this report are not to be construed as an official Department of the Army position unless so designated by other authorizing documents.

REPORT DOCUMENTATION PAGE

Form Approved
OMB No. 0704-0188

1. REPORT DATE *(DD-MM-YYYY)*	2. REPORT TYPE	3. DATES COVERED *(From - To)*
XX-01-2008	Final	May 2006 - May 2007

4. TITLE AND SUBTITLE

Evaporation into Couette Flow

5a. CONTRACT NUMBER
DAAD13-03-D-0017

5b. GRANT NUMBER

5c. PROGRAM ELEMENT NUMBER
SAIC Agreement No. 669338

6. AUTHOR(S)

Danberg, James E. (SAIC)

5d. PROJECT NUMBER

5e. TASK NUMBER

5f. WORK UNIT NUMBER

7. PERFORMING ORGANIZATION NAME(S) AND ADDRESS(ES)

SAIC, P.O. Box 3465A, Box Hill Corporate Drive, Abingdon, MD 21009

8. PERFORMING ORGANIZATION REPORT
ECBC-CR-092

9. SPONSORING / MONITORING AGENCY NAME(S) AND ADDRESS(ES)
DIR, ECBC, ATTN: AMSRD-ECB-RT-TD, APG, MD 21010-5424

10. SPONSOR/MONITOR'S ACRONYM(S)

11. SPONSOR/MONITOR'S REPORT NUMBER(S)

12. DISTRIBUTION / AVAILABILITY STATEMENT
Approved for public release; distribution is unlimited.

13. SUPPLEMENTARY NOTES
COTR: Dan Weber, AMSRD-ECB-RT-TD, (410) 436-2158

14. ABSTRACT

The equation governing the evaporation from a microliter droplet of a chemical warfare agent into Couette flow is derived using an integral method. It is assumed that the evaporation from a small drop is controlled by the linear velocity distribution in the near wall region of a laminar or turbulent atmospheric boundary layer. The result is presented in terms of nondimensional parameters: Sherwood (Sh) number as a function of Reynolds (Re) number to the 2/3 power, and Schmidt (Sc) number to the 1/3 power with a 0.852 constant of proportionality. These results are confirmed using a Crank-Nicolson implicit solution of the diffusion equation. In addition to agreement between the integral and numerical results for the diffusion rate, good agreement is also obtained in the computed concentration distributions with the profiles assumed in the integral analysis. Evaporation rate predictions are compared to evaporation rate measurements of HD droplets on a glass surface obtained in the U.S. Army Edgewood Chemical Biological Center 5-cm wind tunnels. The average slope of the Sh number data versus the Re number Sc number parameter is 0.98, which exceeds the theoretical results by 13%, but the prediction falls within two standard deviations of $\pm 17\%$.

15. SUBJECT TERMS

Computational Fluid Dynamics (CFD)	Boundary-layer	Dimensional Analysis	Agent fate
Secondary evaporation	Reynolds Number	Schmidt Number	HD
Integral Theory	Linear sublayer	Sherwood Number	

16. SECURITY CLASSIFICATION OF:			17. LIMITATION OF ABSTRACT	18. NUMBER OF PAGES	19a. NAME OF RESPONSIBLE PERSON
a. REPORT	b. ABSTRACT	c. THIS PAGE			Sandra J. Johnson
U	U	U	UL	32	19b. TELEPHONE NUMBER *(include area code)* (410) 436-2914

Standard Form 298 (Rev. 8-98)
Prescribed by ANSI Std. Z39.18

Blank

PREFACE

The work described in this report was authorized under Contract No. DAAD13-03-D-0017. The work started in May 2006 and was completed in May 2007.

The use of either trade or manufacturers' names in this report does not constitute an official endorsement of any commercial products. This report may not be cited for purposes of advertisement.

This report has been approved for public release. Registered users should request additional copies from the Defense Technical Information Center; unregistered users should direct such requests to the National Technical Information Service.

Acknowledgments

The author wishes to acknowledge the indispensable help and encouragement provided by D. J. Weber, Research and Technology Directorate, U.S. Army Edgewood Chemical Biological Center, and M. Miller, W. Shuely, R. Nickol, B. King, J. Pence, and C. Franklin, Science Applications International Corporation, Abingdon, MD. Dan Weber provided overall direction to the project and access to a broad range of the 5-cm tunnel data. Miles Miller made the evaporation rate data included in this report available. Wendel Shuely provided the thermodynamic data on the HD Agent and did valuable service in researching the related literature. Robert Nickol, Bruce King, and John Pence conducted the experimentation that generated the evaporation data used in this report. Christine Franklin is also acknowledged for her assistance in formatting this document for publication.

Blank

CONTENTS

FIGURES

TABLES

EVAPORATION INTO COUETTE FLOW

1. INTRODUCTION

1.1 Objective

The objective of this report is to present a theory for the evaporation of a small drop into a Couette flow. The application of such an analysis is to the experimental data obtained from the Agent Fate 5-cm wind tunnels for hazardous chemicals and comparison with some of that data is provided to assess the usefulness of the analysis. The ultimate purpose being to develop secondary evaporation models for evaluating the effects of routine industrial emissions, accidental releases of hazardous materials, and dissemination of chemical and biological warfare agents.

One of the problems in modeling of the evaporation of chemical agents into the atmosphere is in determining the way evaporation depends on the wind speed. Full-scale atmospheric tests are difficult to get reliable data from because of the large number of variables that cannot be controlled. Wind tunnel tests can provide data under controlled conditions and theoretical analysis can provide the relationships needed. A number of investigators have studied these problems and examining some of their results is in order.

But before beginning the review it is necessary to state that the discussion will be limited to small surface drops of a few microliters. Excluded are the large-scale spills where normal boundary layer techniques are more applicable.

Only two-dimensional flows will be considered here. This restriction means that the evaporation, subsequent diffusion, and the main flow velocity vector remain in one plane normal to the surface; thus, lateral diffusion and cross flows are assumed negligible.

Here the primary concerned is the relationship between the evaporation rate and the variables that affect it such as drop size and drop properties. Of particular interest is the effect of the convective external flow on the evaporation rate. Ultimately, there is also concern with the time-history of the decreasing mass of the drop and its changing geometry; but, this is not addressed here.

1.2 Dimensional Analysis

Dimensional analysis can be used to present the evaporation rate in terms of three dimensionless parameters, Sherwood number (Sh), Reynolds number (Re), and the Schmidt number, (Sc). The set of basic variables are:

- N = Evaporation rate, Kg/$m^2 s$
- $\overline{N}$ =Average drop evaporation rate, $Kg/m^2 s$, $= \dot{M}/A$
- $\dot{M}$ = Total drop evaporating mass flux, Kg/s
- A = Evaporating surface area, m^2
- D = Mass diffusion coefficient, m^2/s
- ν = Kinematic viscosity, m^2/s
- L = A characteristic length, m
- u= A characteristic velocity, m/s
- $c_w - c_\Delta$ = The concentration difference in Kg/m^3 of the evaporating vapor between the surface, w, and the edge of the evaporating vapor dispersion layer, Δ
- C = Proportionality constant

The result is:

$$Sh = C\,Re^n\,Sc^m \qquad (1)$$

where

$Sh = \dfrac{N \cdot L}{(c_w - c_\Delta) \cdot D}$, Sherwood number

$Re = \dfrac{uL}{\nu}$, Reynolds number

$Sc = \dfrac{\nu}{D}$, Schmidt number

1.3 Literature Review

Table 1 presents the results of a brief search of available evaporation rate estimates. The first three items are from a survey by Barry.[1] It is interesting that none of the empirical methods are concerned with the diffusivity of the evaporated vapors. The first four include vapor properties through the surface concentration or vapor pressure. All of the empirical and the two theoretical boundary layer methods apply to large spills. A problem with applying the large spill and boundary layer approach is the fetch or boundary layer development length that is difficult to define in an atmospheric environment. Only the Baines and James[2] and the present prediction specifically address the droplet case.

The Baines and James paper is basically identical to the present work, which was carried out independently. The only differences are that they used a similarity solution technique, and their method of averaging to obtain the final result was to match the circular area to a square to get the stream wise droplet dimension of $L=\sqrt{\pi/4}d$.

Table 1. Evaporation Rate Formula Cited in the Literature

Reference	Evaporation Rate	n	m	Notes
	Empirical			
U.S Air Force[3]	$N \propto u^{0.75} M_w T_F \left(P_{vp}/P_{vp,Hy}\right)$	0.75		P_{vp} sat. vapor pres.
EPA[4,5]	$N \propto u^{0.78} M_w^{0.667} P_{vp}/RT_A$	0.78		P_{vp} sat. vapor pres.
Stiver-MacKay[6,7,8,9]	$N \propto uP_{vp}M_w/RT_A$	1.0		P_{vp} sat. vapor pres
Sutton[10]	$N \propto u^{0.78} L^{0.11} (c_w - c_\infty)$	0.78		u=wind vel. L=Free liquid surface
Coutant and Penski[11]	$R_{cp} = R_{cp,0}(1 + c\,Re^q (h/H)^p)$	0.63		$R_{cp} \propto \dot{M}$ u=Ave. duct vel. H=duct height
	Theoretical			
Laminar boundary layer[12]	$\overline{Sh}_L = 0.66\,Re_L^{1/2}\,Sc^{1/3}$	1/2	1/3	u=free stream L=b.l. development
Turbulent boundary layer[12]	$Sh_L = 0.036\,Re_L^{4/5}\,Sc^{1/2}$	4/5	½	u=free stream L=b.l. development
Discontinuous Boundary conditions[13]	$\overline{Sh}_d = 0.334\,Re_d^{1/2}\,Sc^{1/3} \cdot \left[\frac{3}{2}\left(\frac{4}{3}\right)^{1/3}\left(\frac{d}{L}\right)^{1/6}\right]$	1/2	1/3	d=drop dia. u=free stream Vel. L= b.l. dev.
Baines & James[2]	$\overline{Sh}_L = 0.840\left[\frac{u_{\tau L}}{\nu}\right]^{\frac{2}{3}} Sc^{1/3}$	2/3	1/3	u_τ=Friction Vel. L=drop length
Present	$\overline{Sh}_d = 0.852\left[\frac{u_\tau d}{\nu}\right]^{\frac{2}{3}} Sc^{1/3}$	2/3	1/3	u_τ=Friction Vel. d=drop dia.

2. DROPLET CONFIGURATION

Figure 1 shows measurements of three droplets on glass. The configuration appears to closely approximate a segment of a sphere depicted as the arc of a circle. In free-fall with negligible aerodynamic effects, the drop will form a perfect sphere as its minimum energy configuration. In fact that is how the "initial" diameters are obtained.

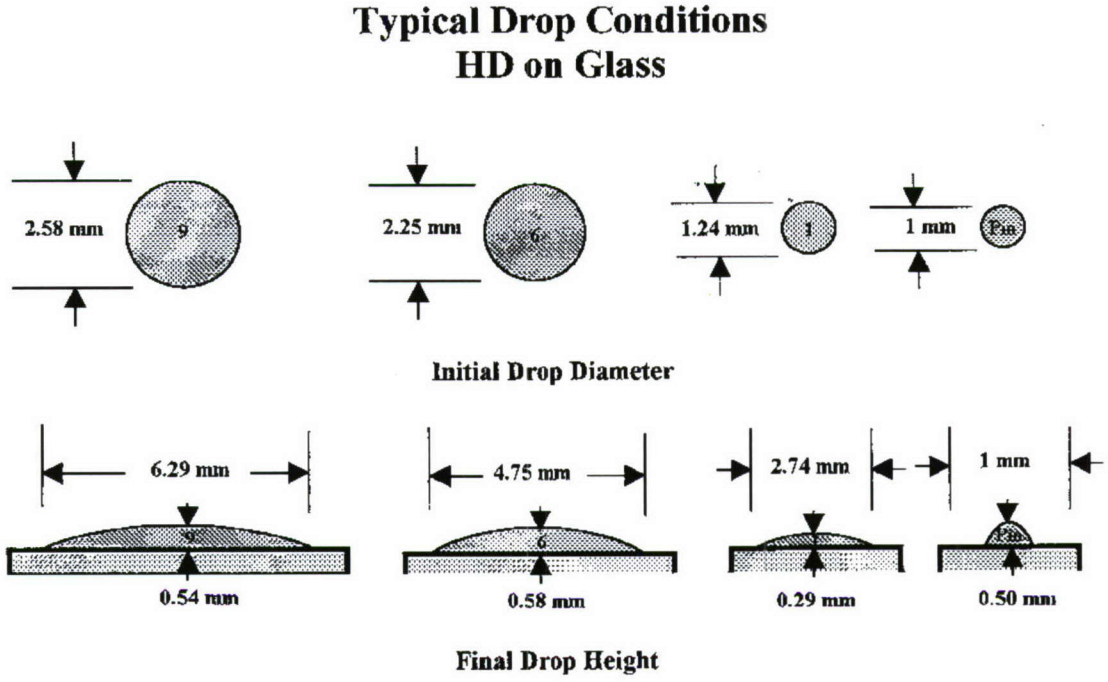

Figure 1. Configuration of Three Sessile Drops

The present case is quite different in that the drop is acted upon by gravity on a solid surface. Surface tension must still be a part of picture. A new effect is the action of surface tension in the vicinity of the surface. A molecule on the droplet surface at the junction of the liquid, gas and solid has the solid molecule's attraction to contend with. This produces a contact-angle that may be considered a property of the system.

If we assume the shape of the droplet to be a segment of a sphere then the radius of curvature is dictated by the contact angle and the volume of the liquid. Unfortunately, not enough is known about the properties of the liquid and the liquid on glass to calculate the configuration from this basic approach but the contact angle can be calculated from the given measurements of surface diameter d and droplet height h. All the important characteristics of the droplet can be defined in terms of d and the parameter $\eta = \frac{h}{d}$.

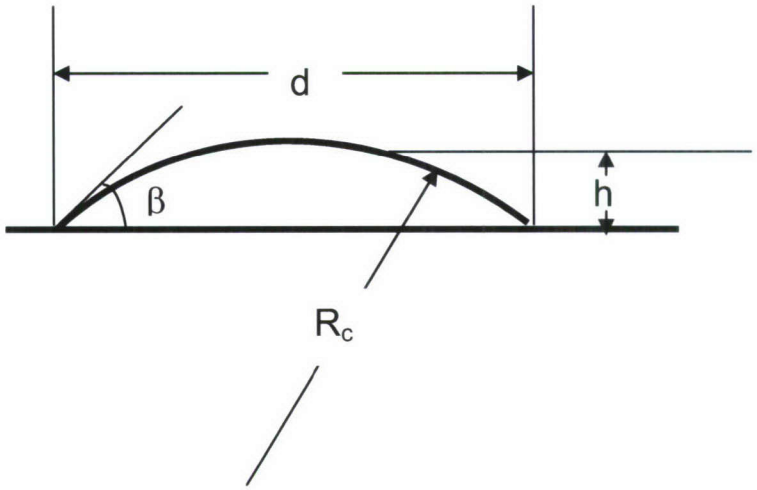

Figure 2. Sketch of Droplet Geometry

First the radius of curvature of the surface droplet, R_c, is

$$R_c = \frac{d}{8}\left[\frac{1}{\eta} + 4\eta\right] \tag{2}$$

The contact angle, β, is

$$\beta = \arctan\left(\frac{4\eta}{(1-4\eta^2)}\right) \tag{3}$$

We see that if β is a constant then η = h/d is also a constant independent of the volume. The average of the experimental data is $\eta = 0.1046 \pm 20\%$ and the value of h/d using $23.6^\circ \pm 4^\circ$ is also 0.1046. Using this value for h/d, the base diameter (chord in cross section) of the spherical segment can be written in terms of h/d and the volume, Q, of the droplet.

$$d = \left[Q/\left\{\frac{\pi}{6}\eta\left(\frac{3}{4} + \eta^2\right)\right\}\right]^{1/3} \tag{4}$$

Finally the surface area of the segment can be calculated

$$A_{seg} = \frac{\pi d^2}{4}\left[4\eta^2 + 1\right] \tag{5}$$

The data obtained from Figure (1) is provided in Table 2.

Table 2. Measured Values				
Q cu mm	9	6	1	Average
d mm	6.29	4.75	2.74	
h mm	0.54	0.58	0.29	
h/d	0.0858	0.1221	0.1058	0.1046
β Deg. Equation (2)	19.5	27.4	23.0	23.6
R mm Equation (1)	9.428	5.153	3.381	

The calculations, based on β, for the three droplets are given in Table 3. Included are calculations of the wetted area, $\pi d^2/4$, which shows the relatively small error that would be made in neglecting the curvature of these small droplets. This also provides a check that the curved surface area is correctly calculated.

Table 3. Calculated Values				
Q cu mm	9	6	1	Average
d mm Equation (4)	5.999	5.2411	2.884	
d (meas.)/d (cal)	1.0484	0.9063	0.8500	0.9682
R_c mm, Equation (1)	9.428	5.153	3.381	
A_{seg} sq mm, Equation (5)	30.32	23.14	7.01	
A Droplet Wetted Area, sq mm	28.27	21.57	6.53	

Since the diameter in the segment area formula is proportional to a segment volume raised to the 1/3 power then the area of the segment is proportional to the 2/3 power of the volume. The proportionality factor is just a function of h/d. We can write the area as

$$A_{seg} = f\left(\frac{h}{d}\right)Q^{2/3} \qquad (6)$$

The result is plotted in the Figure 3. If the contact angle varied by 5 degrees, the $f(\eta)$ could vary by 20% and the evaporation rate changes proportionatly. Data on the effect of temperature on contact angle of HD are not currently available.

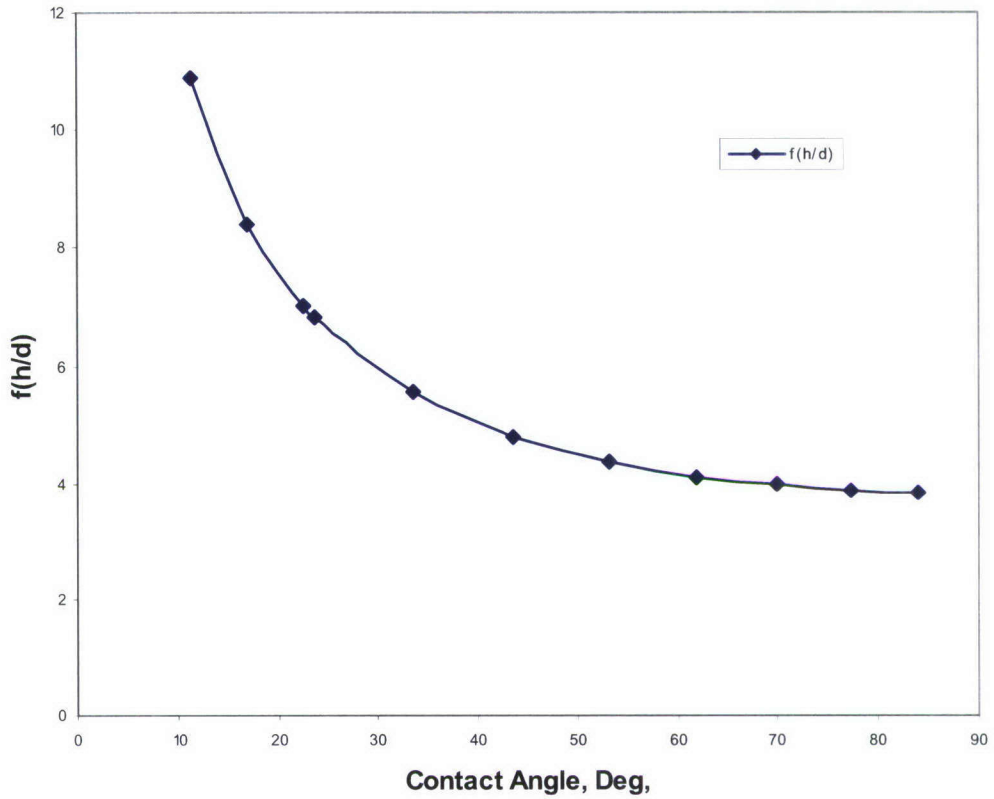

Figure 3. Shape Factor as a Function of Contact Angle

3. DERIVATION OF INTEGRAL THEORY

In this derivation the protuberance of the droplet into the boundary layer will be neglected. The largest drop in the thinnest boundary layer considered for the 5-cm tunnel tests extends as far into the flow as the thickness of the linear region of the sublayer. Because the droplet can be considered slender (d/h $\cong$ 10) the boundary layer can ride smoothly over the drop. However, the magnitude of the approximation made by neglecting the disturbance has not been determined.

It is also assumed that the evaporation rate is determined by the concentration distribution in the vicinity of the droplet and that the vapors from the droplet are confined to the linear sublayer at least as an approximation. It is further assumed that the vapors added are so dilute that they do not change the composition of the main gas flow or produce a significant change in the sublayer momentum flow field.

For example the displacement effect of the added gas does not change the velocity field. The sublayer is modeled as Couette flow with the same normal velocity gradient as the turbulent sublayer.

$$\left(\frac{du}{dy}\right)_{Turb,sl} = \frac{u_\tau^2}{\nu} = \left(\frac{u_H}{H}\right)_{Couette} \qquad (7)$$

where u_H is the moving upper wall velocity at a distance H from the fixed wall. The same integral procedure as that used for the temperature step boundary condition problem in heat transfer[12] is used here.

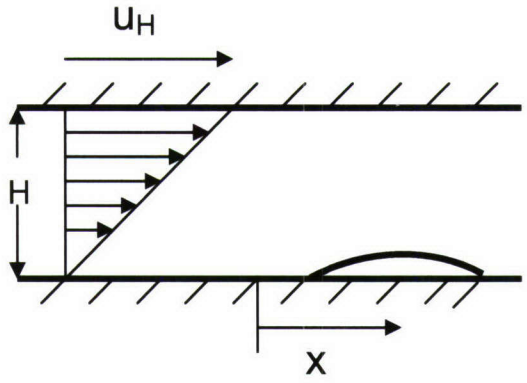

Figure 4. Sketch of Droplet in Couette Flow

The first element is to define the concentration thickness, ϑ.

$$(c_w - c_H)u_H\vartheta = \int_0^{\Delta} ucdy \tag{8}$$

It should be noted that c_H just denotes the concentration of the evaporated vapor present in the ambient air but not coming from the droplet (thus, in this case, it is zero). It is assumed uniform in all the oncoming flow.

The velocity distribution is

$$u = u_H \frac{y}{H} \tag{9}$$

In this boundary analysis the droplet and the concentration distribution are taken as two-dimensional to simplify the development. The concentration distribution is assumed as in the simple laminar boundary layer:

$$c = (c_w - c_H)\left[1 - \frac{3}{2}\frac{y}{\Delta} + \frac{1}{2}\left(\frac{y}{\Delta}\right)^3\right] \tag{10}$$

Let $\varsigma = \frac{y}{\Delta}$ where Δ is the penetration depth of the vapor concentration. Combine these relations so that ϑ becomes

$$\vartheta = \frac{\Delta^2}{H}\int_0^1 \left[\varsigma - \frac{3}{2}\varsigma^2 + \frac{1}{2}\varsigma^4\right] = \frac{\Delta^2}{H}\frac{1}{10} \tag{11}$$

The next step is to relate the rate of change of ϑ with respect to the longitudinal coordinate x with the wall boundary condition. Note it is assumed that $x = 0$ defines the start of the two-dimensional drop.

$$(c_w - c_H)u_H \frac{d\vartheta}{dx} = -D\left(\frac{dc}{dy}\right)_{y=0} = N \tag{12}$$

where D is the diffusion coefficient of the vapor in air and N is the mass flux per unit area of vapor from the fixed wall. Using the definitions of ϑ and c and recognizing that $\Delta(x)$ is the only function of x.

$$\frac{1}{5}\frac{u_H}{H}\Delta\frac{d\Delta}{dx} = \frac{3}{2}\frac{D}{\Delta} \tag{13}$$

This differential equation can be solved using the initial condition that $\Delta = 0$ at x=0 to give

$$\Delta = \left[\frac{45}{2}\frac{Dx}{u_H/H}\right]^{1/3} \tag{14}$$

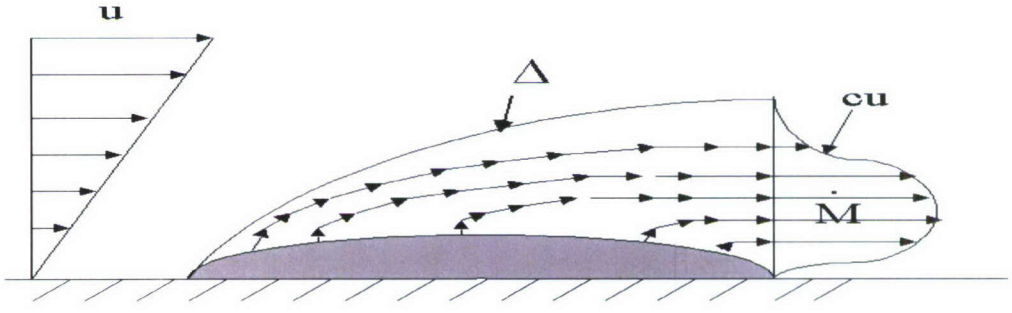

Figure 5. Sketch Depicting the Flow of Evaporated Vapor

The next step is to use this result (Equation (14)) in the definition of ϑ (Equation (11)) and put these into the left-hand-side of Equation (12) to define N.

$$N = C(c_w - c_H)D\left[\frac{Dx}{u_H/H}\right]^{-1/3}\ ;\ \mathbf{C} = \frac{2}{30}\left(\frac{45}{2}\right)^{2/3} = 0.531 \qquad (15)$$

Equation 15 can be put into nondimensional form of an Sherwood number, Sh_d, where the length scale is the diameter of the drop, d. The right-hand-side contains a sublayer Re number where we will use Equation (7) to replace u_H/H by u_τ^2/ν. The diffusivity, D, divided into the air kinematic viscosity forms the Sc number, $Sc = \nu/D$.

$$Sh_d = \frac{Nd}{(c_w - c_H)D} = C\left[\frac{u_\tau d}{\nu}\right]^{\frac{2}{3}} Sc^{1/3}\left(\frac{x}{d}\right)^{-1/3} \qquad (16)$$

Evaluation of an average $\overline{\overline{Sh}}$ may be obtained by integrating over x/d from 0 to 1.

$$\overline{\overline{Sh_d}} = \frac{\overline{\overline{Nd}}}{(c_w - c_H)D} = \frac{3}{2}C\left[\frac{u_\tau d}{\nu}\right]^{\frac{2}{3}} Sc^{1/3},\ \ \frac{3}{2}C = 0.796 \qquad (17)$$

This is the simple averaging over the droplet diameter or taking the averaging on the centerline of the actual drop. The actual drop is circular in wetted area on the surface.

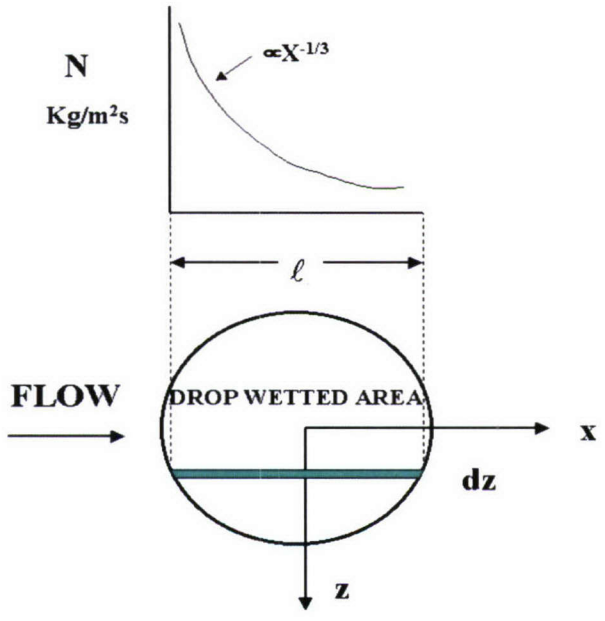

Figure 6. Integration over the Droplet

A better approximation to the effect of the circular geometry is to consider integrating over the actual area of the drop as illustrated in Figure 6.

$$\frac{\pi d^2 \overline{N}}{4} = \dot{M} \propto 2 \int_0^{d/2} \int_0^{\ell} N dx dz \qquad (18)$$

the z coordinate is in the surface perpendicular to the normal x-y plane.

where $\left(\frac{\ell}{2}\right)^2 + z^2 = \left(\frac{d}{2}\right)^2$ (19)

And if $N \propto \left(\frac{x}{d}\right)^{-1/3}$ then $\overline{N} = 1.07 \overline{\overline{N}}$ or in nondimensional terms.

$$\overline{Sh}_d = 0.852 \left[\frac{u_\tau d}{\nu}\right]^{\frac{2}{3}} Sc^{1/3} \qquad (20)$$

This is the final result, which shows the appropriate Re number can be based on the shear velocity and the droplet diameter.

The ratio of Δ at the trailing edge of the drop to the actual thickness of the laminar sublayer can now be computed. The linear sublayer thickness is taken as $y^+ = 4$, corresponding to a 1 % deviation from the linear velocity distribution. If we call this point δ_{sl} then

$$\frac{\Delta}{\delta_{sl}} = \frac{1}{4}\left(\frac{45}{2}\right)^{1/3} Sc^{-1/3} \left[\frac{u_\tau d}{\nu}\right]^{\frac{1}{3}} , \quad \frac{1}{4}\left(\frac{45}{2}\right)^{1/3} = 0.706 \qquad (21)$$

4. CFD COMPUTATION OF COUETTE FLOW EVAPORATION

The numerical computation of the evaporation from a sessile drop into a Couette flow has been undertaken as a first step in applying numerical techniques to the case of turbulent boundary layers including three-dimensional diffusion effects. This problem is basically the same as described for the integral method.

The numerical code used is a modification of a program published by Morgan[14] for computation of unsteady one-dimensional heat transfer. The solution technique is an implicit Crank-Nicolson method with two-point boundary condition and marches in x from an initial condition.

4.1 Diffusion Equation

The equation to be studied here is the diffusion equation, which for the two-dimensional case in a Couette flow is:

$$u\frac{\partial c}{\partial x} = D\frac{\partial^2 c}{\partial y^2}, \text{ on the drop } c(x,y=0)=c_w,\ c(x,\ y\to\infty)=0 \qquad (22)$$

where y is the distance normal to the surface and x is the distance down stream on the drop. D is the diffusivity and u is assumed linear in y for Couette flow.

In such a flow $u = \frac{u_\tau^2}{\nu} y$; thus, the governing equation differs from the heat transfer equation because of a variable coefficient involving y. Since the penetration depth of the vapor is in practice finite, the second boundary condition is simplified to a sufficiently large constant y.

Equation (22) can be put into the form:

$$Y\frac{dC}{dX} = \frac{d^2C}{dY^2}, \qquad (23)$$

where $Y = \frac{u_\tau y}{10\nu}$, $X = \frac{u_\tau x}{1000\nu Sc}$, and $C = \frac{c}{c_w}$

The boundary conditions are Y=0, C=1 at the surface of the drop and Y = 1, C=0 at y^+ = 10 assuming this value of y^+ is sufficient away from the vapor plume. The initial condition at X = 0, C=0 for all Y except at Y=0, C=1 corresponding to a step in the initial boundary condition at the drop.

4.2 Finite-Difference

Equation (23) can be written in finite-difference form using central differences in both directions but with the node taken at the mid point of the X step. Taking i to be the ith step in X and j in Y.

$$[Y_j]\cdot\left(\frac{C_{i+1,j}-C_{i,j}}{\Delta X}\right) = \frac{1}{2}\left(\frac{C_{i+1,j+1}-2C_{i+1,j}+C_{i+1,j-1}}{(\Delta Y)^2}\right)+\frac{1}{2}\left(\frac{C_{i,j+1}-2C_{i,j}+C_{i,j-1}}{(\Delta Y)^2}\right) \qquad (24)$$

The unknowns are in the i+1 X step where there are three unknown $C_{i+1,j-1}$, $C_{i+1,j}$, and $C_{i+1,j+1}$. The square bracketed term is the only addition to the code developed by Morgan. It is convenient to define a combined step variable r.

$$r = \frac{\Delta X}{(\Delta Y)^2} \tag{25}$$

The three unknowns have coefficients a, b, c and the remainder d.

$$a = -\frac{r}{2},\ b = Y_j + r,\ \text{and}\ c = -\frac{r}{2} \tag{26}$$

$$d = (Y_j - r)C_{i,j} + \frac{r}{2}(C_{i,j+1} + C_{i,j-1}) \tag{27}$$

A tridiagonal matrix is constructed from the a, b, c and d's for j=2 to N-1 and the two boundary conditions at j=1 and N. The Thomas algorithm can be used to determine all of the N-2 unknowns in C at each X step and as the solution marches downstream the entire concentration distribution is defined.

4.3 Stability

The Crank-Nicolson implicit scheme is stable for any step size in a wide range of problems that vary smoothly and not too rapidly. It may be viewed as a Fourier series representation of the solution where if the function varies rapidly or is discontinuous. The series involves many high frequencies. It is the high frequencies that are unstable in the Crank-Nicolson method. A way of making it more stable is to reduce the step to meet the stability criterion of the explicit techniques that is $r \leq 0.5$. As the solution moves away from a discontinuity the step size can be increased to a more efficient value.

4.4 CFD Results

The application of the Morgan code is to that of a two-dimensional drop of HD, which extends 0.006 m stream-wise in a Couette flow of friction velocity, u_τ=0.2 m/s and kinematic viscosity of 0.0000159 m^2/s. The surface concentration of HD is 0.002 Kg/m^3 and Sc number is 2.53 from which the diffusivity of HD in air can be calculated.

The drop stream-wise dimension (designated d in analogy with the drop surface diameter) is considered the maximum distance in x to be computed. When it is put into the nondimensional form suggested by Equation (23), X is 0.02983 at d. Initially 40 steps were selected, which results in an ΔX=0.00075. A y^+ of 10 was thought to be sufficient to define the outer boundary condition of c=0. Two hundred steps in Y were assumed or ΔY = 0.005.

The evaporation rate, N (in Kg/$m^2 s$), can be determined by Fick's Law.

$$N = -D\left(\frac{\partial c}{\partial y}\right)_w \tag{28}$$

In terms of the computational variables, Equation (28) can be most easily rewritten in nondimensional Sherwood number terms. (Note the length d makes Sh_d nondimensional but N and Sh_d are still functions of x.)

$$Sh_d = \frac{Nd}{c_w D} = Re_d[C(1) - C(NYOUT)]/[10(NYOUT - 1)DY] \tag{29}$$

where $Re_d = u_\tau d/\nu$ and NYOUT is the j step used to calculate the concentration derivative (≥ 2 and is not sensitive to the choice because of the linearity near the surface.) Figure 7 illustrates the distribution of Sh_d versus the computational X. The line drawn through the data was calculated by taking a point near X=0.03 and running a curve through that point proportional to $X^{-1/3}$ as predicted by the integral technique and the similarity theory of Baines and James.[13]

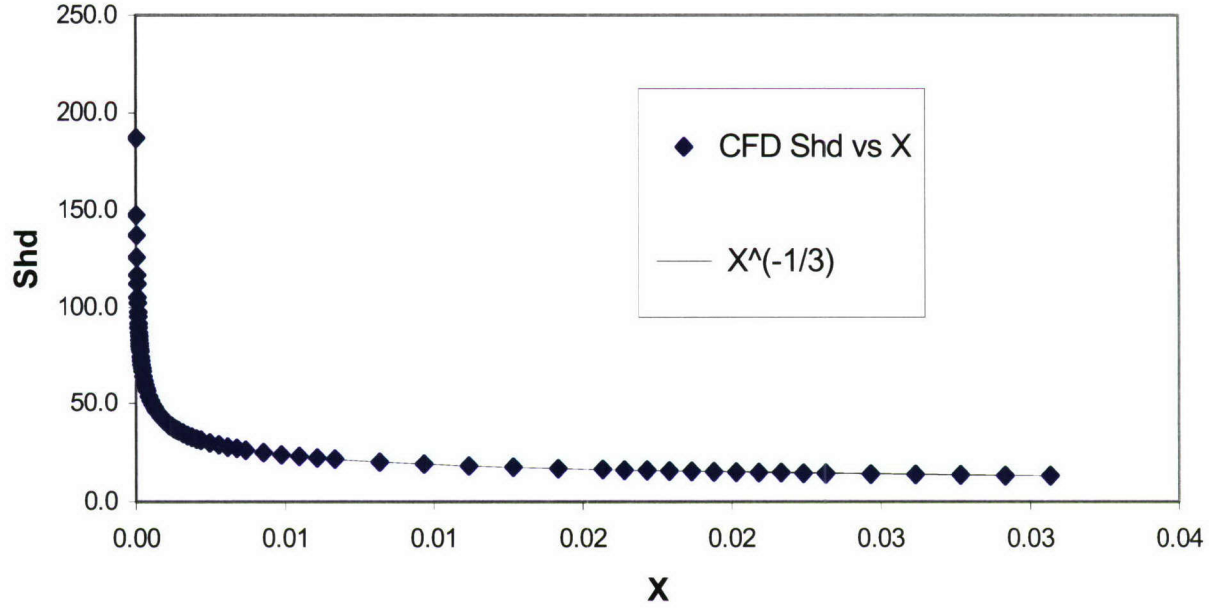

Figure 7. Local Sherwood Number versus Computational X

Figure 8 more definitively confirms that the CFD results duplicate the results of the integral analysis and that of reference 2. The line designated as "Integral" is Equation (16). The CFD data differ from Equation (16) only at the smallest values

of x/d, but this is the region of the steepest gradient in the distribution and the region of the greatest uncertainty in the numerical computation.

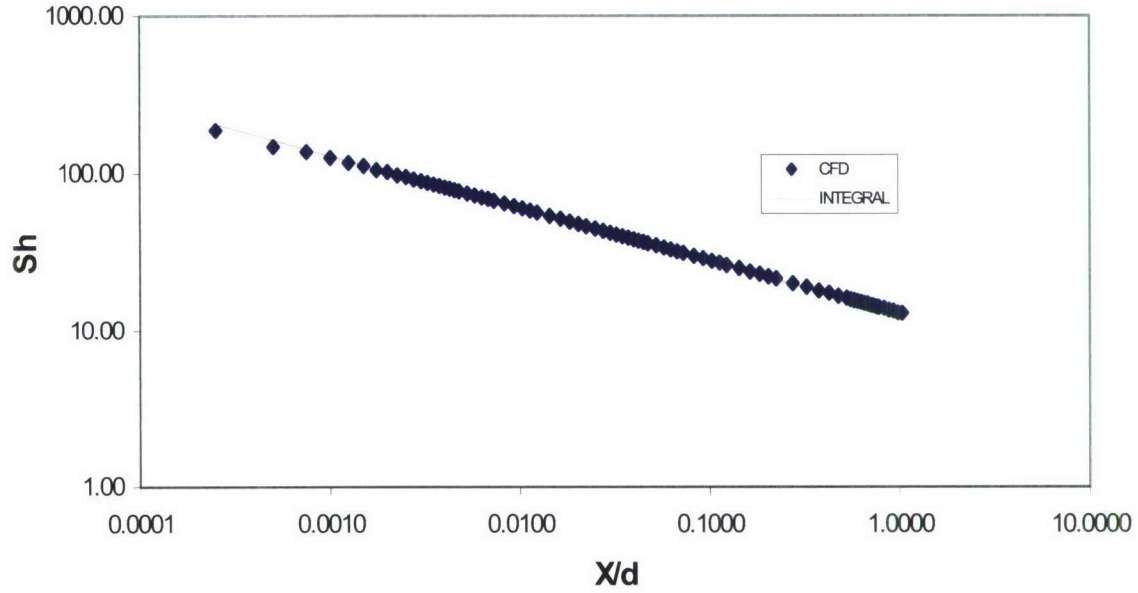

Figure 8. Comparison between CFD and Integral Analysis

Concentration profiles can be obtained from the numerical computation and examples of a few profiles are given in Figure 9. The four profiles are specified in terms of the numerical x variable X but the corresponding x/d's, i.e., the distance from the leading edge in percent of the assumed drop diameter (6 mm) are given in Table 4.

Table 4. Comparison of CFD and Integral Theories

X	x/d (%)	$\frac{\Delta}{d}$ (%)	Sh_d (CFD)	Sh_d (Integral)
0.000427	1.43	2.8	53.2	53.2
0.00157	5.25	4.3	34.5	34.5
0.00817	27.40	7.5	19.9	19.9
0.0307	100.00	11.6	12.8	12.9

Also shown on Figure 9 are profiles computed from Equation 10 of the integral theory. And the penetration thickness Δ is given by:

$$\Delta = d\left[\frac{45}{2}\frac{1}{Sc\,Re_d^2}\frac{x}{d}\right]^{1/3} \qquad (30)$$

which is a rewritten form of Equation (14). Values of the penetration thickness as a percent of the diameter are tabulated in Table 4.

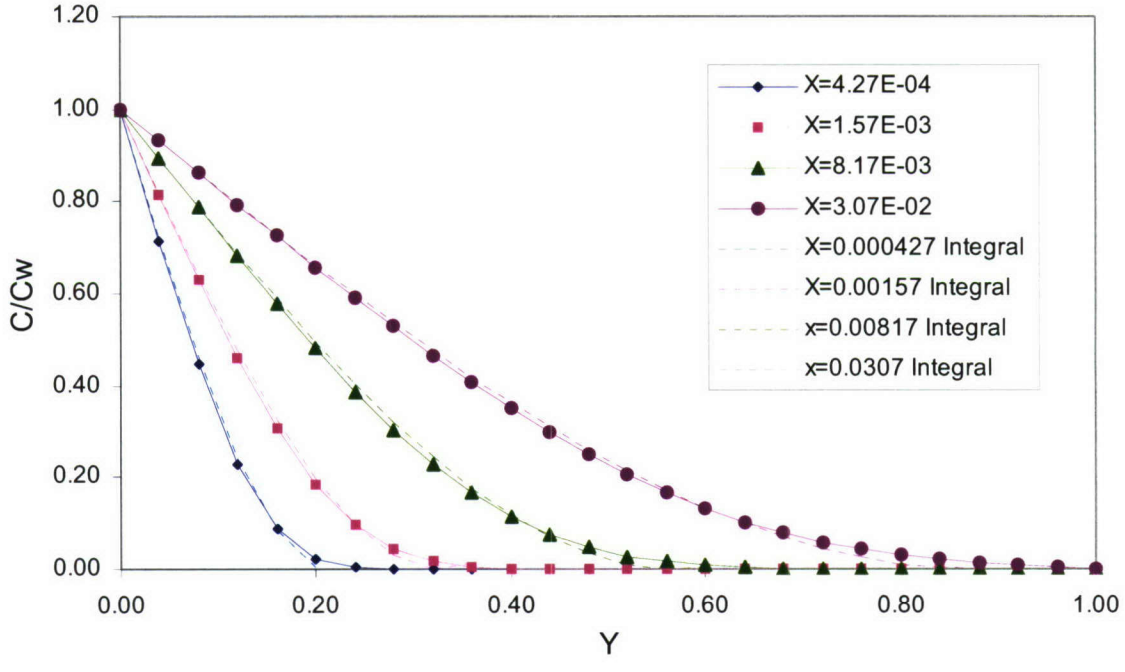

Figure 9. Concentration Profiles

It is apparent from Figure (9) that the integral assumption closely approximates the correct CFD profile. This is confirmed by comparison of the calculated Sh numbers that may be viewed as nondimensional normal concentration gradients at the surface (see Equations (28) and (29).) The calculated Sh numbers from the CFD and Integral theories are given in Table 4 and are in almost perfect agreement.

5. COMPARISON WITH EXPERIMENTAL DATA

Information is available which provides data on HD diffusivity and its partial pressure as a function of temperature.[15]

5.1 Properties of HD

The values determined are given in Table 5. To convert partial pressure into concentration, the molecular weight is required and a value based on the chemical

formula $C_4H_8Cl_2S$, which gives a Molecular weight = 159.07 Kg/Kmole. Thus, the gas constant becomes $R_{HD} = 52.27 \frac{Nm}{KgK}$. The perfect gas formula, Equation (31), was used to calculate the concentration listed in Table 5.

$$c_w = \frac{p_{HD}}{R_{HD} T} \tag{31}$$

where the pressure, p_{HD}, is the saturation vapor pressure of HD. The temperature is the absolute ambient temperature. The concentration of HD in the free-stream is taken as zero. Also given in Table 5 are the values of Sc number.

Table 5. Properties of HD

Temperature °C	Vapor Pressure N/m^2	Concentration c_{HD}, Kg/m^2	Diffusivity m^2/s	Sc No. Sc
0	1.32			
15	5.01	0.000333	5.50E-06	2.65
20	9.20			
25	14.66			
35	32.4	0.002013	6.50E-06	2.53
40	46.66			
50	105.4	0.00643	7.00E-06	2.55

5.2 Comparison with Data

Measurements[16] are available of the total evaporation, $\dot{M}$, in micro g/min in the 5x5 cm tunnels versus the nominal free-stream velocity for three droplet volumes (9, 6, 1 cu mm) and for three tunnel system temperatures (15, 35, 50 °C.) The drops considered here are all for HD on a glass surface. Tabulated data are provided in the attached Table 6. The areas and diameters of the droplet are taken from previous discussion of the droplet configuration. Sutherland's dynamic viscosity formula was used. The density was calculated from the specified temperature and standard atmospheric pressure of 101.325 KPa. In Table 5 the average friction velocity for the three speed ranges were taken from the recent evaluation of the velocity profiles[17] in the 5-cm tunnels.

The Sh number, Sh, data are graphed versus the combined parameter, $Re^{2/3}Sc^{1/3}$, in Figure 10, with temperature as a parameter, including the over-all correlation line (linear statistical best fit.)

The slope b of Sh ($=y_i$) versus $Re^{2/3}\,Sc^{1/3}$ ($=x_i$) has been computed using the conventional method for a correlation assumed to go through the origin: that is summing over the N=19 data pairs:

$$b=\frac{\sum_i y_i}{\sum_i x_i} \tag{32}$$

and the standard deviation in the y data relative to the best fit line is:

$$\sigma_y=\sqrt{\frac{1}{N-1}\sum_i (y_i-bx_i)^2} \tag{33}$$

The standard deviation in the slope is obtained by the propagation of error method.

$$\sigma_b=\sqrt{\sum_i\left(\frac{\partial b}{\partial y_i}\sigma_y\right)^2}=\sigma_y\sqrt{\frac{N}{(\sum_i x_i)^2}} \tag{34}$$

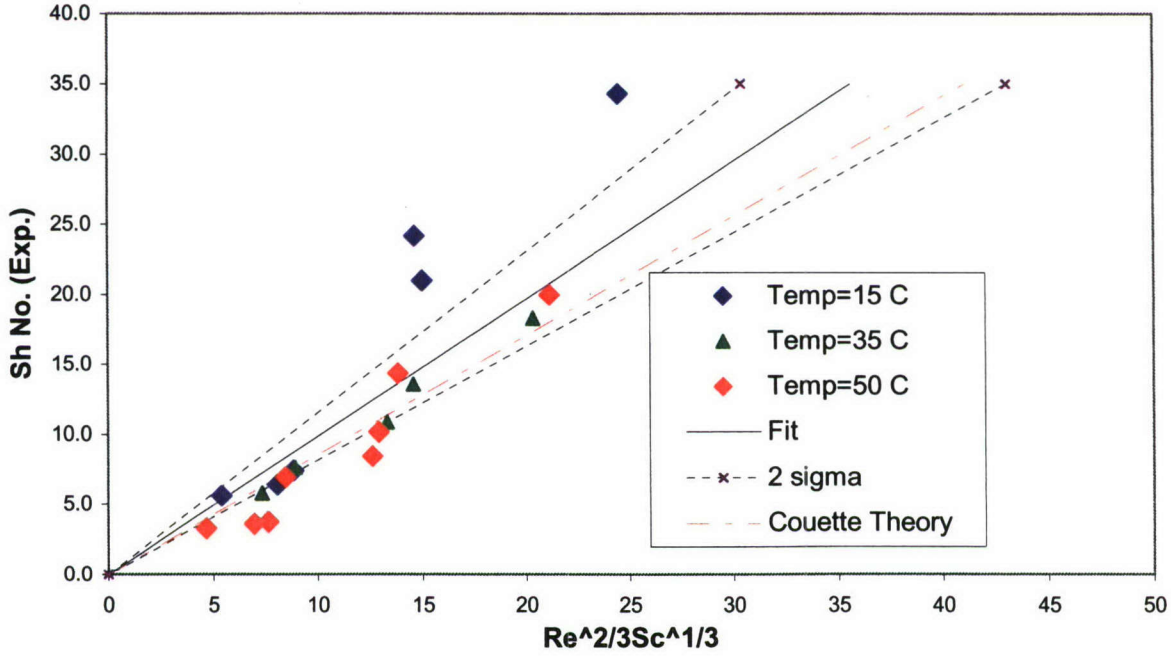

Figure 10. Evaporation Rate Correlation

The experimental result is a slope of 0.98 ±17%; whereas, Equation (20) predicts that the slope of the line should be 0.852 or 13% smaller. However, it should be kept in mind that the analysis is for the simpler two-dimensional case whereas the drop concentration distribution is actually three-dimensional. That is the concentration, in the three dimensional case, is free to defuse latterly from the drop as well as normal to the wall.

Also on the figure is the uncertainty band based on plus or minus 1.96 sigma or a confidence level of 95%. The upper and lower slope of this band are ± 17% of the best fit value of 0.98 and is affected by some of 15 °C data, which fall considerably outside of the band. If these points were omitted from the statistical analysis the resulting best-fit slope would be 0.83 or about 2.5% lower than the predicted value.

Some of the inaccuracies may be due to the vapor pressure and diffusivity values that were obtained from graphical data. Or the uncertainty in the actual drops size and area that may be affected by temperature that has not been accounted for in these results. There is scatter in all the measurements but somewhat more in the 15 °C data as might be expected.

6. CONCLUSIONS

By developing a theory for the evaporation from a droplet under conditions appropriate to the Fate wind tunnel an attempt has been made to show that a relatively simple Couette diffusion-convection model could provide a correlation formula that would generalize the specific test measurements (at different droplet volume, temperature and different sublayer shear velocity.)

The CFD code, modified to solve the 2-D Couette flow evaporation problem, provides identical results as the integral theory and the similarity theory of Baines and James.

The CFD calculation provides reliable details to the solution unavailable to the approximate theories

The CFD approach has the prospect of extension to three dimensions and into a turbulent boundary layer.

The resulting correlation as exhibited in Table 6 and Figure 10 bring the Couette theory into a certain level of agreement with the experimental data. The slope in the statistical best-fit line is 0.98, which is 13% higher than the Couette theory's value of 0.852. The theory's slope falls slightly above the lower 2-sigma uncertainty band and if the three high 15 °C data were omitted as outliers the best-fit slope would be 0.83 or 2.5% below the prediction.

There seems to be a slight trend in the data at the higher velocities: that is, higher Re numbers tend to increase faster than the linear correlation.

This model indicates that the shear velocity and droplet diameter are the appropriate length and velocity scales for the evaporation in this case. There is also reason to think that the temperature effects can be understood through the incorporation of the temperature dependent thermodynamic properties of the droplet material.

Table 6a. Input Data

T	Q	M dot	u delt	u tau	A	d	D	nu	c surface
C	milli l	micro g/min	m/s	m/s	sq mm	m	sq m/s	sq m/s	Kg/cu m
15	9	4.1	0.22	0.0393	30.3	0.006	5.50E-06	1.46036E-05	0.000333
15	9	19	3.61	0.181	30.3	0.006	5.50E-06	1.46036E-05	0.000333
15	6	3.1	0.2	0.0393	23.1	0.00524	5.50E-06	1.46036E-05	0.000333
15	6	11.7	1.61	0.096	23.1	0.00524	5.50E-06	1.46036E-05	0.000333
15	1	1.5	0.26	0.0393	7.01	0.00288	5.50E-06	1.46036E-05	0.000333
15	1	5.6	3.61	0.181	7.01	0.00288	5.50E-06	1.46036E-05	0.000333
35	9	53.7	1.6	0.096	30.3	0.006	6.50E-06	1.64466E-05	0.002013
35	6	20	0.2	0.0393	23.1	0.00524	6.50E-06	1.64466E-05	0.002013
35	6	37.6	1.61	0.096	23.1	0.00524	6.50E-06	1.64466E-05	0.002013
35	6	63.2	3.58	0.181	23.1	0.00524	6.50E-06	1.64466E-05	0.002013
35	1	14.5	1.61	0.096	7.01	0.00288	6.50E-06	1.64466E-05	0.002013
50	9	51.2	0.22	0.0393	30.3	0.006	7.00E-06	1.78814E-05	0.00643
50	9	196	1.6	0.096	30.3	0.006	7.00E-06	1.78814E-05	0.00643
50	9	272	3.61	0.181	30.3	0.006	7.00E-06	1.78814E-05	0.00643
50	6	42.8	0.2	0.0393	23.1	0.00524	7.00E-06	1.78814E-05	0.00643
50	6	100.2	1.61	0.096	23.1	0.00524	7.00E-06	1.78814E-05	0.00643
50	1	21.6	0.26	0.0393	7.01	0.00288	7.00E-06	1.78814E-05	0.00643
50	1	45.6	1.61	0.096	7.01	0.00288	7.00E-06	1.78814E-05	0.00643
50	1	66.9	3.61	0.181	7.01	0.00288	7.00E-06	1.78814E-05	0.00643

Table 6b. Nondimensional Parameters

T	Q	Sh=	Re	Re^2/3	Sc	Sc^1/3	R2/3S1/3	(yi-b*xi)^2
C	milli l	yi					xi	
15	9	7.39E+00	16.14666	6.388347	2.66E+00	1.384733	8.846156	0.391307
15	9	3.42E+01	74.36503	17.68395	2.66E+00	1.384733	24.48755	145.3124
15	6	6.40E+00	14.10142	5.836805	2.66E+00	1.384733	8.082418	0.85128
15	6	2.42E+01	34.44621	10.58671	2.66E+00	1.384733	14.65977	118.189
15	1	5.61E+00	7.750397	3.91636	2.66E+00	1.384733	5.423114	0.483348
15	1	2.09E+01	35.69521	10.8411	2.66E+00	1.384733	15.01203	53.83475
35	9	1.35E+01	35.02249	10.70446	2.53E+00	1.36266	14.58653	0.109575
35	6	5.78E+00	12.52127	5.392195	2.53E+00	1.36266	7.347726	0.76985
35	6	1.09E+01	30.58631	9.780282	2.53E+00	1.36266	13.32719	1.461168
35	6	1.83E+01	57.66794	14.92644	2.53E+00	1.36266	20.33966	0.027031
35	1	7.59E+00	16.8108	6.562342	2.53E+00	1.36266	8.942238	0.262752
50	9	3.75E+00	13.18687	5.581631	2.55E+00	1.366998	7.630081	9.971887
50	9	1.44E+01	32.2122	10.12388	2.55E+00	1.366998	13.83933	3.365859
50	9	1.99E+01	60.73341	15.45083	2.55E+00	1.366998	21.12126	0.657115
50	6	3.60E+00	11.51653	5.099737	2.55E+00	1.366998	6.971333	7.399759
50	6	8.42E+00	28.13198	9.249826	2.55E+00	1.366998	12.6445	9.230393
50	1	3.29E+00	6.329697	3.421805	2.55E+00	1.366998	4.677602	0.905171
50	1	6.94E+00	15.46185	6.206418	2.55E+00	1.366998	8.484165	0.560445
50	1	1.02E+01	29.15204	9.472093	2.55E+00	1.366998	12.94834	2.409719
	sum yi=	2.25E+02					sigmaY=	4.448426
						sum xi=	229.371	
						b(slope)=	9.82E-01	
						sigma b=	0.082282	

Blank

LITERATURE CITED

1. Barry, J. "Estimating Rates of Spreading and Evaporation of Volatile Liquids," CEP, January 2005, pp 32-39.

2. Baines, W. D. and D. F. James. "Evaporation of a Droplet on a Surface," Ind. Eng. Chem. Res., 1994, 33, pp 411-415.

3. U. S. Environmental Protection Agency, Federal Emergency Management Agency (FEMA) and U. S. Department of Transportation, Handbook of Chemical Hazard Analysis Procedures, Washington D. C., 1989.

4. U. S. EPA and FEMA. "Technical Guidance for Hazards Analysis," Equation 7, Section G-2, Appendix G, Washington, D. C., December 1987.

5. U. S. Environmental Protection Agency. "Risk Management Program Guidance for Offsite Consequence Analysis," Publication EPA-550-B-99-009, Section D.2.3, Appendix D, Equation D-1, Washington, D. C., April 1999.

6. Stiver, W., and MacKay. "A Spill Hazard Ranking System for Chemicals," Environment Canada First Technical Spills Seminar, Toronto, Canada, 1993.

7. Clewsell, H. J. "A Simple Method for Estimating The Source Strength of Spills of Toxic Liquids," Energy Systems Laboratory, ESL-TR-83-03, 1983.

8. Ille, G., and C. Springer. "The Evaporation and Dispersion of Hydrazine Propellants from Ground Spills," Civil and Environment Engineering Development Office, CEEDO 712-78-30, 1978.

9. Kahler, P., et al. "Calculating Toxic Corridors," Air Force Weather Service, AWS TR-80/003, 1980.

10. Sutton, O. G. Micrometeorology, McGraw-Hill, New York, 1953.

11. Coutant, R. W., and E. C. Penski. "Experimental Evaluation of Mass Transfer from Sessile Drops," I&EC Fundamentals, vol. 21, pp 250, 1982.

12. Kays, W. M., Crawford, M. E. *Convective Heat and Mass Transfer, 3rd Ed.*, McGraw-Hill, New York, 1993.

13. Danberg, J.E. Untitled memorandum to D. Weber and M. Miller ECBC November 11, 2005.

14. Moran, J. "An Introduction to Theoretical and Computational Aerodynamics," Wylie and Sons, 1984.

15. Abercrombie, Patrice. Physical Property Data Review of Selected Chemical Agents and Related Compounds: Updating Field Manual 3-9. ECBC-TR-294, September 2003.

16. Shuely, W.; Nickol, R.; King, B.; Pence, J.; Giannaras; C., D'Onofrio, T.; Donnelly, T.; Durst, D. Fundamental Laboratory Measurements of the Environmental Fate of Chemical Agents on Surfaces. In "Environmental Fate of Chemical Agents; Final Report for DTO CB.42," ECBC-TR-532, U. S. Army Edgewood Chemical Biological Center, Aberdeen Proving Ground, MD, September 2007.

17. Danberg, J. E. Evaluation of 5-cm Agent Fate Wind Tunnel Velocity Profiles, ECBC-CR-091, U.S. Army Edgewood Chemical Biological Center, Aberdeen Proving Ground, MD, September 2007.

NOMENCLATURE

A	Surface Area of evaporating drop (also used to denote an matrix)
a, b, c, d	Coefficients in the tridiagonal matrix
b	Best-fit slope
C	Proportionality constant or Computer variable= c / c_w
c_H	Ambient concentration not from the drop (assumed zero in this study)
c_w	Concentration of vapor at the surface of drop
d	Diameter of sessile drop
D	Diffusivity of evaporated vapor in air
H	Channel height
h	Height of sessile drop
ℓ	x-direction chord of circular surface droplet at z from centerline
L	Characteristic length
$\dot{M}$	Total drop evaporation rate
M_w	Molecular weight
n	Number of data points
N	Local evaporation rate per unit area
$\overline{N}$	Average evaporation rate per unit area= $\dot{M} / A$
$\overline{\overline{N}}$	Average 2-D droplet evaporation rate based on stream-wise dimension
P	Pressure
Q	Volume of drop
R	Gas Constant
R_c	Sessile drop radius of curvature
R_{cp}	Coutant and Penski evaporation parameter $\text{mass}^{2/3}$ /time
$R_{cp,o}$	Coutant and Penski evaporation parameter zero convection velocity
Re_d	Reynolds Number = ud/ν
r	Computer step size parameter = $\Delta X /(\Delta Y)^2$
Sc	Schmidt Number = ν/D
Sh_d	Local Sherwood Number = $Nd/ c_w D$
$\overline{\overline{Sh}}_d$	Average Sherwood Number over drop diameter = $\overline{\overline{N}} d/ c_w D$
$\overline{Sh}_d$	Average Sherwood Number over circular drop area = $\dot{M} d/A c_w D$
T	Temperature
u	Stream-wise velocity
u^+	Law of the wall velocity coordinate = u/u_τ
u_τ	Shear velocity= $\sqrt{\nu\left(\frac{\partial u}{\partial y}\right)_w}$

X	Computer variable= $u_\tau x/(1000\nu Sc)$
x	Coordinate in the flow direction
x_i	Statistical analysis independent variable
x_o	Boundary layer development length
Y	Computer variable= $y^+/10$
y	Coordinate normal to the surface
y^+	Law of the wall coordinate variable = $u_\tau y/\nu$
y_i	Statistical analysis dependent variable

Greek Symbols

β	Contact angle of sessile drop
ϑ	Concentration thickness
Δ	Evaporated vapor penetration distance in y
δ	Boundary layer thickness
η	h/d
ν	Air kinematic viscosity
ρ	Air density
σ	Standard deviation
ς	y/Δ

Subscripts

A	Ambient conditions
b	Slope
F	Correction factor
H	Channel height
HD	Chemical agent $C_4H_8Cl_2S$
i, j	Computer indices in x, y direction
Seg	Segment
sl	Sublayer
vp	Saturation vapor pressure
vp,Hy	Saturation vapor pressure of Hydrazine
y	deviation from best fit line